

Building a Flexible and Economical Voltage-to-Digital Converter for Medical Equipment

KAMEPALLI UMA¹, M SREENU²Assistant professor^{1,2}

DEPARTMENT OF ELECTRONICS AND COMMUNICATION ENGINEERING

P.B.R.VISVODAYA INSTITUTE OF TECHNOLOGY & SCIENCE

S.P.S.R NELLORE DIST, A.P , INDIA , KAVALI-524201

Abstract:

Many electrical and electronic devices used in modern hospitals produce significant levels of interference in the form of background electromagnetic radiation (EMR), which is used by medical staff for calibration and monitoring of therapeutic processes. Sensitive instruments are subjected to additional strain because of the wide range of environmental factors present in a clinical setting. Instrumentation utilized in such settings must be somewhat resistant to these influences if accurate, reproducible, and reliable data are to be obtained. Analog instruments are very vulnerable to noise and temperature fluctuations. Sensors often produce an analogue current or voltage, and it has been shown that converting them early on to a robust digital format would have significant overall benefits to the measurement process. In this paper, we provide a simple and inexpensive method for analog-to-digital conversion working with volt-level signals. It has been successfully implemented in handheld radiation dosimetry instruments used in a variety of clinical settings, and it provides an increase in signal resolution of more than an order of magnitude compared to conventional analog approaches.

INTRODUCTION

The need to detect X-ray fields in our labs motivated the development of the device described in this study, which uses plastic organic scintillator materials that are almost tissue equivalent as the sensor element. These sensors generate very low levels of light that, even when interfaced with the most sensitive of photodiodes, only produce output currents in the nanoamp area, making them unsuitable for usage in clinical situations where beam energies in the KVp range are utilised. Even when paired with a highly insulated buffer amplifier, the system's output is still barely in the microvolt range. Elevating such signals to a level where sufficient resolution could be reached, together with the possibility of capturing and storing the data, posed unique challenges. For used in a controlled laboratory setting, signal measurement devices can be accurate for measuring moderate to high levels of signal [1, but they may lack stability and resolution for measuring extremely low levels of signal]. Our studies led to the creation of a portable apparatus that can accurately detect near tissue equivalent radiation doses in clinical dosimetry settings [2, 3].

The technical implementation of the system is outlined in the following sections. Ambient temperature, vibration, unexpected fluctuations in power supply voltages, and the like have a significant impact on analog circuitry. Signals of interest may easily be overwhelmed by unwanted interference from these and other sources, as well as by the superfluous EMR created by nearby clinical equipment like X-ray generators, linear accelerators, and general control and computer systems. Without a certain degree of performance and stability at the front end, achieving consistent very low level analogue amplification outside of a lab environment is very difficult.

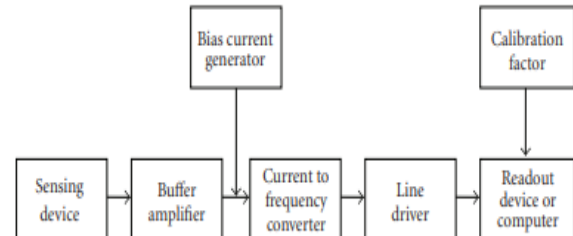


Figure 1: Block diagram showing overview of concept and signal processing chain.

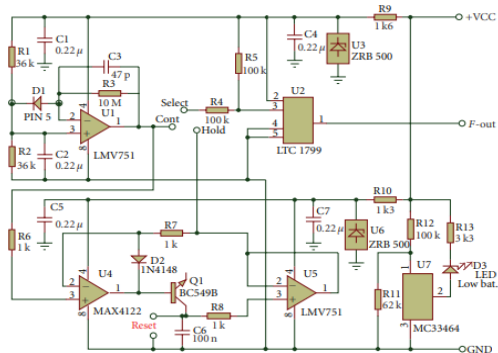


Figure 2: Schematic diagram of a prototype instrument used for scintillation counting.

Once the signal is converted to digital format at a later stage, any errors or spurious responses made during the earlier stages cannot be distinguished

from the desired signal. Since each analogue stage added its own level of instability and self-generated noise, the desired signal information was lost in the noise floor of the additional circuitry, making it impossible to achieve reliable analogue amplification and filtering at the ultra low sensor outputs encountered. To get around this problem, researchers looked into the possibility of early conversion to a digital signal format; however, the high cost of multibit converters able to resolve signals at microvolt levels and the system-generated noise from available PC-based A to D converters made this approach impractical. Due to the lack of an appropriate and cost-effective "off the shelf" system that could be adapted to the task at hand, a novel technology was developed to directly interface a variety of sensor elements and provide a dependable and low-cost method of capturing and storing the resulting data stream. The technique developed and implemented has been shown to significantly enhance the noise immunity of low-level measuring instruments, while also providing significant improvements to system stability in hostile environmental conditions.

FACTORS TO CONSIDER IN CIRCUIT DESIGN

For the goal of direct connection to a wide range of sensors, the following describes the proposal and development of an integrated system for microvolt-level analogue-to-digital conversion utilizing commercially available low power integrated circuit technology. Figure 1 provides a conceptual overview of the topic at hand. Using this idea as inspiration, engineers set out to create a workable piece of electronics. Figure 2 is a typical prototype's design, which demonstrates how analog circuitry has been pared down to the bare minimum necessary for proper termination of the sensing device. A reliable response may be achieved with an analogue input signal current of less than a microamp at the first stage device U2. Figure 2 depicts a specific setup for a scintillation counter that makes use of a photodiode sensor. Pin 3 of U2 receives the buffered voltage from the sensor via a resistance chosen to inject the necessary amount of current. An adequate baseline may be established with the use of a bias current generator, which supplies a constant current. U4 and U5 aren't essential to the conversion process, but they were introduced so that users of handheld instruments would have access to a typical sample and hold facility that would enable them to take a "snapshot" of the data stream at any point in time. Using this supplementary feature does not interfere with the continuous flow of information being processed and stored by a connected PC. Q1's base collector

junction is utilized for preventing reverse voltage and level shifting; a low leakage diode might be employed in its stead. U7 is a battery status indication that may be left out if the instrument is to be powered by an external source.

RESOLUTION OF SIGNALS

Because any drift in the DC bias level arising from the buffer stage would be additive and indistinguishable from the desired input signal, it was necessary to quantify the level of residual noise from the analogue stage as well as its stability over time in order to establish resolution, accuracy, and repeatability of measurements. The testing and measurements were conducted using a UDT PIN 5DPI precision photodiode. After collecting this information, we were able to calculate the sensitivity and margins of error of the current-to-frequency transformation. A high-precision temperature-compensated laboratory standard, which may be considered sufficiently stable for the purposes of providing a reference current source for the instrument, was used to generate the precise reference level used to establish the base frequency of the current-to-frequency converter stage. After letting the sealed instrument case warm up for 15 minutes so that all of the internal circuits could reach thermal equilibrium, a precision data acquisition system with a base resolution of 100 V was used to measure the voltage from the buffer stage to a 10 000 input resistor to the current-to-frequency converter. The photodiode was shielded from the sun throughout this test. The input voltage noise floor and drift of the instrument's input stages were recorded, and the outcomes are shown graphically in Figures 3 and 4 below, keeping in mind the appropriate but limiting factor of the 100 V resolution for the measurement equipment. These noise voltages, denoted by the function $E(t) = 10,000I(t)$, are proportional to the input current to the current-to-frequency converter step. After initial component thermal stability has been achieved, the baseline drift drops to a very low level, as shown in Figure 3 at about 19 Hz/min. That's a drift rate of around 0.02% every minute for the signal being sent out. As most clinical measurements are likely to be taken for less than a minute, this drift would be negligible. The horizontal bands shown in Figure 4 are not due to the buffer or frequency conversion, but rather are an artifact of the lowest resolution (100 V) attainable from the data collecting device utilized to capture this data. The worst case peak-to-peak spread of 3.87 mV reveals the random nature of the overall circuit and incidental noise. Since both positive and negative deviations tend to cluster around a central value,

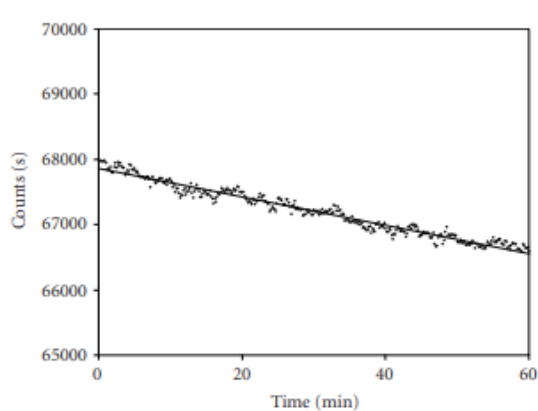


Figure 3: Baseline drift over a period of one hour after thermal stability achieved.

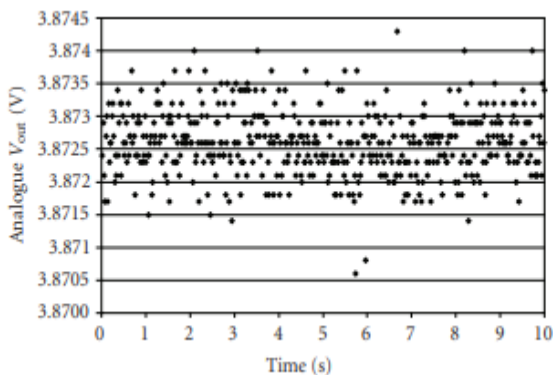


Figure 4: Noise measurements at output from analogue stage V_{out} versus.

Time. 10 second recording at 50 Hz sample rate (500 readings). Note: Output voltage from the analogue buffer stage = 3.8726 V which comprises A/D converter bias voltage plus averaged noise voltage component, $E(t)$. Uncertainty (95% confidence limits) = $\pm 44 \mu V$ when measured over a 10 s period. Noise Band (Worst Case): 3.7 mV (i.e., $\pm 1.85 \text{ mV}$).

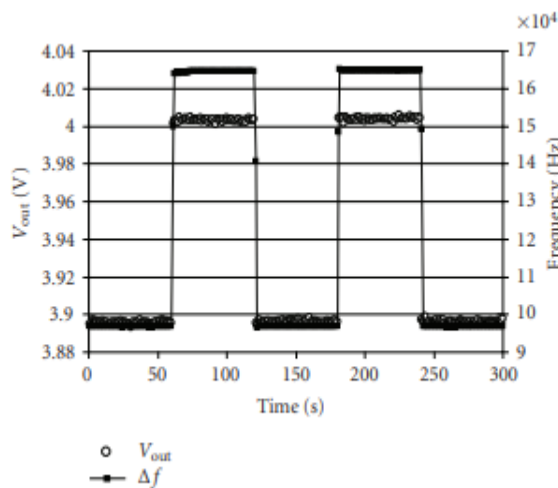


Figure 5: V_{out} from buffer stage versus frequency shift for $\Delta V_{out} = 107.6 \text{ mV}$

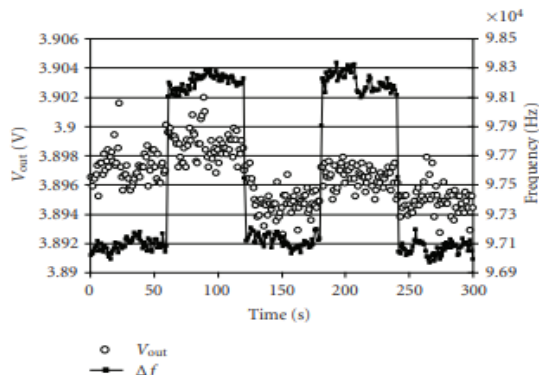


Figure 6: V_{out} from analogue buffer stage versus. Frequency shift for $\Delta V_{out} = 2.0 \text{ mV}$

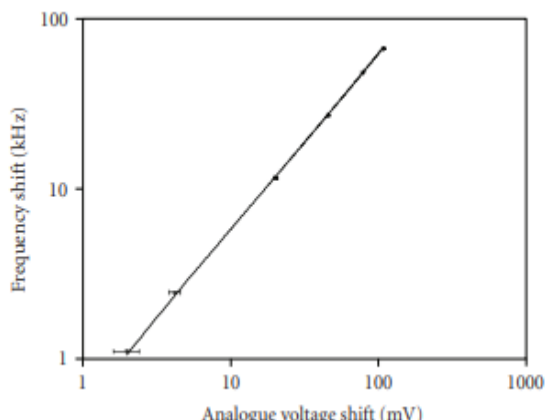
It has been shown that the random negative and positive excursions of the noise component superimposed on the bias voltage which forms the baseline are cancelled out by exploiting the time averaging characteristic which is inherent in the current-to-frequency conversion process. Therefore, the bias voltage can be measured to within 44 V by keeping an eye on it for 10 seconds. Figure 4 shows that the instrument's resolution will be limited by the electronic system's noise floor, which corresponds to an output of 3.87 mV peak to peak from the analogue buffer stage. Using a conservative gain figure of 20x from the buffer stage, the following experiments show that the time-averaging benefit of this design results in a minimum resolution of 44 V, or a sensor delta V output on the order of 2.2 V. The photodiode was used to take a number of measurements while connected to a very dim light source. Figures 5 and 6 demonstrate the results of recording data at regular 5-minute intervals while turning on and off the light source for 1-minute intervals. Figure 5 depicts the situation when a signal of reasonable strength ($V_{out} = 107.6 \text{ mV}$, $f = 67.753 \text{ kHz}$) is applied. In this scenario, we have access to a high degree of precision, and the temporal integration effects inherent to this architecture have a very little impact on resolution.

Figure 6 shows an example where a signal input level of 2.0 mV results in a frequency of 1.117 kHz, which is just above the minimum resolvable level of the noise floor of the analogue stage, demonstrating that time integration in the current-to-frequency conversion stage allows for a stable output frequency to be obtained. The given system was used to compile a table comparing the frequency shift of the current-to-frequency converter's output with the voltage output of the analogue buffer. We took measurements at several points between 2 mV (close to the stage's noise

floor) and 100 mV. Table 1 displays the findings, which are also displayed.

table 1: Analogue output and corresponding frequency shift from A/D conversion using a low-level light source into a PIN 5DPI photodiode. Note the significant improvements in uncertainty factors after processing. (Column 4).

Analogue V_{out} (mV)	% Uncertainty	I-F Frequency Shift (kHz)	% Uncertainty
2.0 ± 0.4	20.0	1.117 ± 0.017	1.5
4.2 ± 0.4	9.5	2.469 ± 0.021	0.85
20.1 ± 0.7	3.5	11.624 ± 0.016	0.14
45.5 ± 0.8	1.8	27.112 ± 0.037	0.14
78.3 ± 0.5	0.64	48.753 ± 0.023	0.05
107.6 ± 0.3	0.28	67.753 ± 0.045	0.07



Analogue voltage shift (mV) 1 10 100 Frequency shift (kHz)
Figure 7: Graph of output Frequency versus. Analogue Voltage output from buffer. Note that this gives a sensitivity of 0.631 kHz/mV = 631 Hz/mV.

as seen in Figure 7, and provide a description of the instrument's response curve. Table 1's values graphically demonstrate the increase in trustworthiness of converted data. At a 2-mV signal, for instance, the level of uncertainty achievable from reading the buffer analogue output is 20% (an unacceptable error figure for any scientific instrument), whereas the level of error is reduced to 1.5% thanks to the significant noise immunity and resolving power provided by this one-of-a-kind digital conversion process. The linearity of the response throughout the expected output range of the electronic systems is consistent with expectations. Therefore, whether one is measuring radiation, light, sound, temperature, magnetic flux, and so on, all that is required is to calibrate the frequency shift observed against a number of reference points for the source. Input buffer amplifiers provide for a wide variety of measurement ranges, limited only by the transducer

of choice. The beta radiation from a Sr-90 brachytherapy source has been measured and profiled using an instrument built according to the specified design and construction, which has shown to be both user-friendly and accurate [3]. The instrument's great sensitivity allowed for the use of a tiny sample size, which

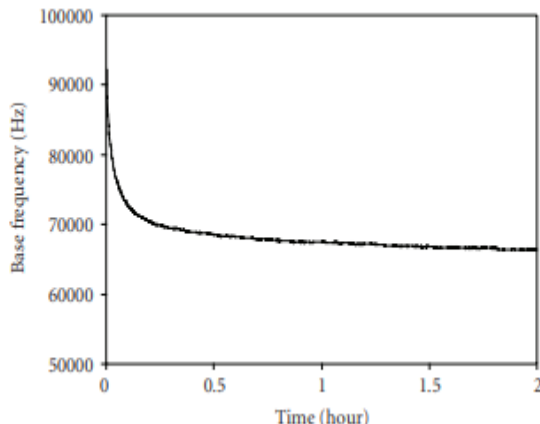


Figure 8: Drift over 2-hour period showing baseline stability attainable after 15 minutes initial warm-up period.

detecting element and, hence, attain spatial resolution of less than 1 mm across the whole radiation field. The Integrated Circuit (IC) LM751 used for input may be swapped out with a single AD626 [6] precision instrumentation differential amplifier in situations where a differential input is necessary for the chosen sensor. This adjustment lowers device-generated noise and improves common-mode rejection, albeit at the expense of some added expense. Figure 8 shows the outstanding baseline stability over time acquired by bench testing a breadboarded circuit based on this idea. This input stage also produced a much better degree of thermal and environmental immunity. When one side of the sensor is not inherently committed to ground, as is often the case in practice, a differential input configuration is the preferred arrangement because it improves overall stability and resolution.

CONCLUSION

The novel signal processing system described herein provides a compact and low-cost method for the capture and integrated digital processing of measurement data in a variety of contexts, including clinical diagnostic and treatment settings, and exhibits a high level of immunity to environmental EMR and internal circuit-generated noise. The method has been proven to provide a resolution boost of at least an order of magnitude compared to conventional A-D converters and analog instruments connected to a PC bus. In addition to its potential incorporation into

laboratory instrumentation, the system's small size and low power consumption make it ideally suited for use in portable battery-operated instruments, where the effects of high levels of environmental noise and interference must be neutralized. The technology has been used effectively in a variety of clinical settings where techniques for detecting and quantifying low levels of radiation were necessary. Direct readout of high intensity photon beams generated by clinical linear accelerators in environments with high levels of background radiation and interference and where remote monitoring at distances of up to 30 meters from the detector is required has been demonstrated by a prototype instrument incorporating this method of signal capture and processing.

REFERENCES

- [1] M. A. Clift, R. A. Sutton, and D. V. Webb, "Water equivalence of plastic organic scintillators in megavoltage radiotherapy bremsstrahlung beams," *Physics in Medicine and Biology*, vol. 45, no. 7, pp. 1885-1895, 2000.
- [2] K. Williams, N. Robinson, J. Trapp, et al., "A portable organic plastic scintillator dosimetry system for low energy X-rays: a feasibility study using an intraoperative X-ray unit as the radiation source," *Journal of Medical Physics*, vol. 32, no. 2, pp. 73-76, 2007.
- [3] M. Geso, N. Robinson, W. Schumer, and K. Williams, "Use of water-equivalent plastic scintillator for intravascular brachytherapy dosimetry," *Australasian Physical & Engineering Sciences in Medicine*, vol. 27, no. 1, pp. 5-10, 2004.
- [4] <http://www.national.com/catalog/>.
- [5] <http://www.linearteck.com/>.
- [6] <http://www.analog.com/product>